1 **Integrated Geophysical Analysis of Rangpur Saddle: Insights on Tectonics and**
2 **Magnetic Mineral Potential of North-Western Bangladesh**

4 Mohammad Tawhidur Rahman Tushar[1], Asif Ashraf[2], Md. Mahfuz Alam[1], Md Nasif Jamil[1], Saba Karim[1],
5 Md. Shahjahan[3], Md. Anwar Hossain Bhuiyan[1]

7 [1]Department of Geology, University of Dhaka, Dhaka-1000, Bangladesh
8 [2]Department of Earth Sciences, University of Oregon, Eugene, Oregon-97401, United States of America
9 [3]Geological survey of Bangladesh, 153 Pioneer Road, Dhaka-1000, Bangladesh

11 *Correspondence to: Mohammad Tawhidur Rahman Tushar (mtrt@du.ac.bd) and Asif Ashraf (aashraf@uoregon.edu)*

13 **Abstract**

15 The northwestern region of Bangladesh holds untapped potential for magnetic mineral deposits at
16 shallow depths. Unlike much of Bangladesh, characterized by thick sediments of Bengal Basin,
17 this area is an extension of the Indian Shield, often referred to as the Stable Platform. It is also
18 geologically distinct, hosting structures related to the breakup of Pangea. The geology and
19 tectonics of this region have remained largely understudied. To address this gap, this study
20 integrates gravity, magnetic, seismic, and drilling data to investigate the subsurface structure and
21 evaluate the resource potential of the area. We utilize advanced filtering and modeling techniques,
22 including tilt derivatives and horizontal gradient methods, to understand the tectonic framework
23 and geometry of the subsurface structures. Our spatial analysis, using multiple geophysical
24 datasets, reveals distinct bipolar magnetic anomalies ~~characterized by alternating magnetic highs and lows~~,
25 which we attribute to gabbroic intrusions along extensional faults that define the region's horst and
26 graben structures. To validate our interpretations, we developed an integrated 2-D subsurface
27 model that aligns with the observed geophysical data. However, the study is limited by the
28 availability of high-resolution seismic data and the sparse distribution of drilling locations, which
29 may affect the precision of our subsurface characterization. Our findings provide crucial insights
30 into the tectonic evolution of the stable platform and underscore the economic potential of the
31 Rangpur Saddle, the shallowest part of the stable platform, for mineral exploration. These insights
32 pave the way for further exploration and development initiatives focused on uncovering the
33 mineral wealth of this underexplored region.

34

35 **1. Introduction**

36

37 The northwestern part of Bangladesh is rich in potential mineral resources. The geological
38 diversity of this area suggests the presence of other valuable minerals that remain largely
39 unexplored (Akhtar, 2005; Hasan et al., 2023; Moon, 2022). In this area, basement rocks are
40 discernible at *[present]* relatively shallow depths of 128 meters, hosting a spectrum of economic mineral
41 resources, including coal, limestone, white clay, and hard rock (Khan & Rahman, 1992). Notably,
42 Pirganj in the Rangpur district (**Figure 1**) records the country's highest magnetic anomaly
43 suggesting the potential for magnetic mineral ore deposits. In the 1990s, drilling activities were
44 conducted in the region after developing a 2D subsurface model by the Geological Survey of
45 Bangladesh (GSB) in collaboration with the United States Geological Survey (USGS). Despite
46 these efforts, no noteworthy ore body was identified during the drilling process (Rahman & Ullah,

47 2009). Moreover, the tectonic evolution of the Paleo-Proterozoic basement in the northwest region
48 of the Bengal Basin still needs to be studied.
49
50 The study area is located in a region commonly referred to as the Rangpur platform or saddle
51 (Masum et al., 2021), an eastern extension of the Indian Shield (Alam et al., 2003). The northern
52 part of the Rangpur Saddle rests on a shallow Precambrian basement, ranging from 130 to 1000
53 meters in depth. This area of Bangladesh is geologically stable, characterized predominantly by
54 horsts and grabens, which were formed during the Cretaceous rifting of the Indian plate from the
55 Antarctica-Australia section of Gondwanaland (Curray, 1991; Curray & Moore, 1974). Although
56 the basement primarily consists of diorite, tonalite, and granodiorite, it is also intersected by
57 pegmatite and mafic/ultramafic dykes (Hossain et al., 2007; Kabir et al., 2001).
58
59 In this study, we explore the possibility of mafic dykes as the source of high magnetic anomalies
60 using multiple geophysical datasets while establishing the regional geological structure of this
61 significantly understudied area. We aim to conduct integrated spatial analysis and develop
62 subsurface models with gravity, magnetic, seismic, and drilling data to understand the regional
63 geological features. Gravity and magnetic data are widely used to understand and characterize
64 geological formations, particularly for identifying thin magnetic layers or faults (Adebiyi et al.,
65 2023; Jaffal et al., 2010). High-resolution potential field data help identify structures related to
66 local-scale mineralization that are covered by shallow alluvium or other unconsolidated sediments
67 (Hendrickson, 2016; McCafferty et al., 2014). Since potential field data can yield multiple
68 solutions (Filina et al., 2019). We also incorporate seismic and drilling data to constrain the
69 subsurface framework and produce more reliable results (Sundararajan, 2012). Our study applies
70 various filters to magnetic and gravity data to enhance and delineate regional crustal structures,
71 with a focus on highlighting structure edges where metallic mineral deposits are likely to be found
72 (Hildenbrand, 2000).
73
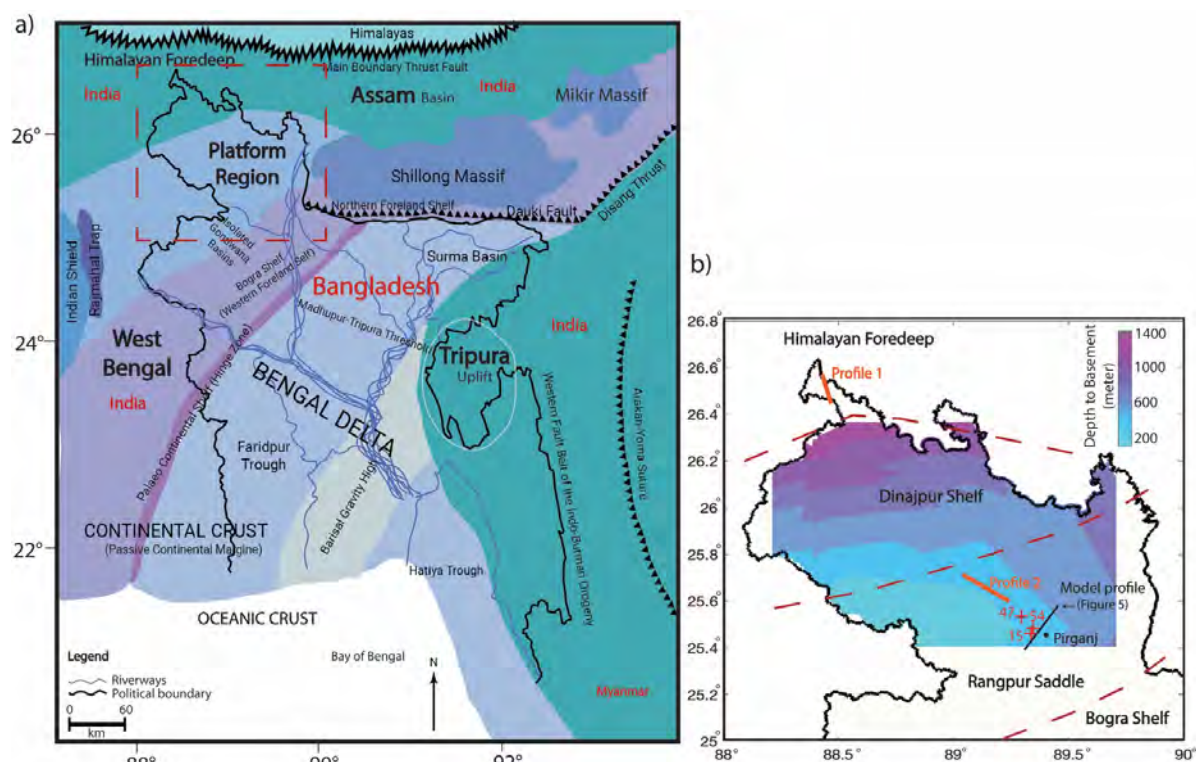
Figure 1: (a) Regional geological map of Bangladesh adopted from Hossain et al. (2019), illustrating various geological and tectonic zones with distinct color coding. The names of neighboring countries are labeled in red. The red dashed box indicates the study area in the northwestern part of Bangladesh. (b) The map of the northwestern Bangladesh region shows basement depth with its tectonic subdivisions. Regional basement depths are collected from GSB and constructed from various seismic reflection surveys. Red dashed lines mark the approximate boundaries of the tectonic divisions. Seismic profiles (orange lines) and drilling locations (red plus signs) utilized in this study are also highlighted. Our specific study area, Pirganj, is also shown on the map, where the highest magnetic anomaly is observed. The integrated 2-D modeling profile of this study is also shown in this map with a solid black line.

2. Geological setting

Bangladesh, though geographically compact, possesses a complex and diverse geological framework shaped largely by its position within the Bengal Basin (Roy and Chatterjee, 2015). This region is primarily divided into two major tectonic units (Morgan and McINTIRE, 1959). To the northwest of the hinge zone (see **Figure 1a** for location), the stable platform region features a shallow basement composed predominantly of Precambrian-aged rocks (Uddin and Lundberg, 1998). Conversely, the southeastern portion of the Bengal Basin comprises a geosynclinal basin, distinguished by significant sediment accumulation, with sediment thicknesses exceeding 12 kilometers (Alam, 1989). This tectonic configuration highlights the geological contrasts between the stable platform and the more dynamic, subsiding basin to the southeast.

The Bengal Basin, encompassing Bangladesh and parts of the neighboring Indian states of West Bengal, Assam, and Tripura, is situated at the northeastern edge of the Indian craton. It is one of

South Asia's largest peripheral collisional foreland basins, with a sedimentary sequence spanning from the Early Cretaceous to the Holocene (DeCelles, 2011). The study area, located in the northwest part of the basin and known as the stable platform, consists of three geological components (Hossain et al., 2019): the Dinajpur Shelf, Rangpur Saddle, and the Bogra Shelf (**Figure 1b**). The Himalayan Foredeep region, located just north of the Dinajpur Shelf, contains the deepest basement in the stable platform (**Figure 1b**) and hosts numerous faults associated with extensional tectonics (**Figure 2a**). South of the Foredeep region, the Dinajpur Shelf gently slopes northward toward the Himalayan Foredeep at an angle of 1-3 degrees and is covered by recent sedimentary deposits. The Rangpur Saddle, the southern block of the Dinajpur Shelf, connects the Indian Shield to the Shillong Plateau and contains the shallowest basement in the Bengal Basin (Jain et al., 2020) (**Figure 1b**). The Bogra Shelf, on the southern slope of the Rangpur Saddle, is formed during the Early Cretaceous rifting of the Indian plate from Gondwana (Alam, 1989; Alam et al., 2003). Both the Rangpur Saddle and Bogra Shelf host several horsts and graben, and half-graben basins (**Figure 2b**).

The entire north-eastern Bangladesh is geologically stable with minimal folding impact that can be traced back from Rodinia and Luna or Colombia supercontinents (Ameen et al., 2007; Zhang et al., 2012). Ameen et al. (2007) suggest that the basement is a separate micro-continental fragment trapped during the northward migration of the Indian Plate, while Hossain et al. (2007) propose that it is a continuation of the central Indian tectonic zone. During the Precambrian, only the stable shelf of the Bengal basin was part of the Indian Plate within Gondwana. By the Middle Jurassic (~170–175 Ma), the Indian Plate began drifting, and becoming isolated by the end of the Paleocene (~55.9 Ma) (Hossain et al., 2019). During the Late Paleozoic–Mid Mesozoic, the stable shelf was developed as an intra-cratonic rift basin with Gondwana sediments in graben structures, followed by Kerguelen igneous activity and widespread Rajmahal Trap volcanism (Hossain et al., 2019; Valdiya, 2016).

The basement in our study area is the shallowest part of the Stable Shelf, which is uplifted to a depth of 128 m from the surface, overlain by the Plio-Pleistocene Dupi Tila Sandstone and Madhupur Clay (Rahman 1987), and is mainly composed of crystalline rocks, including granite, granodiorite, and gneiss (Alam et al., 2003; Hossain et al., 2007). There is no outcrop of Precambrian basement in this area, and the commonly observed horst and graben structures control the stratigraphic subdivision. The Precambrian basement in this region lies beneath thick Cenozoic clastic deposits and is primarily felsic in composition, intersected by mafic-ultramafic and occasional felsic dykes (Chowdhury et al., 2022). Fault-bound graben basins within the basement contain Carboniferous rock units from the Permian Period (286 to 245 million years ago) called Gondwana formation, marking the oldest sedimentary rocks in Bangladesh (Alam et al., 2003; Jain et al., 2020). Above the Permian Gondwana formation is the Jurassic Rajmahal Trap Formation, consisting of volcanic basalt strata (Alam, 1989; Roy and Chatterjee, 2015). The Shibganj Trapwash Formation overlays it, formed through weathering and erosion of the underlying igneous rocks (Khan, 1991).

The Rangpur Saddle serves as the subsurface extension of the Indian shield, stretching between the Shillong Plateau to the east and the Rajmahal Hills to the west. Geophysical studies have identified two major faults framing the Garo-Rajmahal gap: the Dhubri-Jamuna Fault (western edge of Garo Hills) and the Rajmahal Fault (eastern edge of Rajmahal Hills) which encloses the

144   Rangpur saddle (Hossain et al., 2019). Tectonic activities, particularly extensional tectonics during
145   continental rifting, have significantly disrupted the basement topography, forming numerous
146   horsts and grabens (Ahamed et al., 2020; Khan & Rahman, 1992). Despite this, the study area
147   remains predominantly flat with sediment covers (Khan, 1991) from the Pleistocene to Holocene
148   period (Reimann and Hiller, 1993). Near the Rangpur Saddle, the eastern part of the Indian Shield
149   includes three major tectonic domains: Singhbhum Craton, Singhbhum Mobile Belt, and
150   Chhotanagpur Gneissic Complex (Mukhopadhyay and Matin, 2020). Singhbhum Craton is
151   characterized by prolonged crustal evolution during the Archean, comprising lithologies such as
152   granitoids and metamorphic rocks. Singhbhum Mobile Belt underwent accretion and modification
153   through volcanics, dyke swarms, and various intrusive bodies in the Proterozoic. Chhotanagpur
154   Gneissic Complex comprised mainly of gneisses, amphibolites, and granulites with mafic dyke
155   swarms, forming a structurally complex mobile belt. The tectonics of this region can be
156   characterized by intra-cratonic structural depressions between the uplifted tectonic blocks. Seismic
157   reflection studies indicate that the Moho in this region is complex and laminated, suggesting a
158   history of tectonic and magmatic activity (Valdiya, 2016). In the West Bengal basin, the Moho is
159   relatively shallow and horizontal (at a depth of 36 km), while other nearby regions (e.g., Kutch
160   basin) have a dipping Moho influenced by tectonic processes (Rangin and Sibuet, 2017).
161
162   Magnetic minerals, particularly iron ore, are widely found across the Indian Shield. These iron
163   deposits typically appear as metamorphosed banded iron or silica formations. In eastern India, the
164   Precambrian iron ore of the Singhbhum-North Orissa region is a horseshoe-shaped synclinorium
165   that contains the most significant iron deposits near Bangladesh. The first discovery of iron ore in
166   Bangladesh is located on the Dinajpur slope of the Rangpur platform (Alam et al., 2003). Around
167   30 km southwest of our study area, Masum et al. (2021) report iron ore-bearing basement rock
168   about 30 km southwest of our study area, with the iron ores occurring as a thin, metamorphosed
169   laminated layer.
170
171   To understand the geological succession in Pirganj and its surroundings, we present a generalized
172   lithological depiction using data from EDH-15 and GDH-54 drill holes (Table 1).
173
174   Table 1: Stratigraphic Succession of Pirganj & its adjoining Areas according to drill holes EDH-15 and GDH-54
175

Age	Rock Units	Lithology	Thickness (m)
Recent	Alluvium	Loose sand, medium to coarse-grained	52
Unconformity			
Pliocene	Dupitila	Sandstone(SST), silty SST, pebbly SST, pebbly bed; SST: medium to coarse-grained, pebbles: quartzite, gneiss & schist	33
Unconformity			
Late Oligocene to Early Miocene	Surma	Alteration of SST and shales and their combination, sand and silty shale. SST: fine to medium-grained; shale: soft and sticky	125
Unconformity			

Late Cretaceous to Paleocene	Cherra Sandstone	Sandstone: medium to coarse-grained	50
Unconformity			
	Basement	Gabbro; Diorite, quartz diorite, granodiorite, quartz monazite.	180+ (base not seen)

176
177
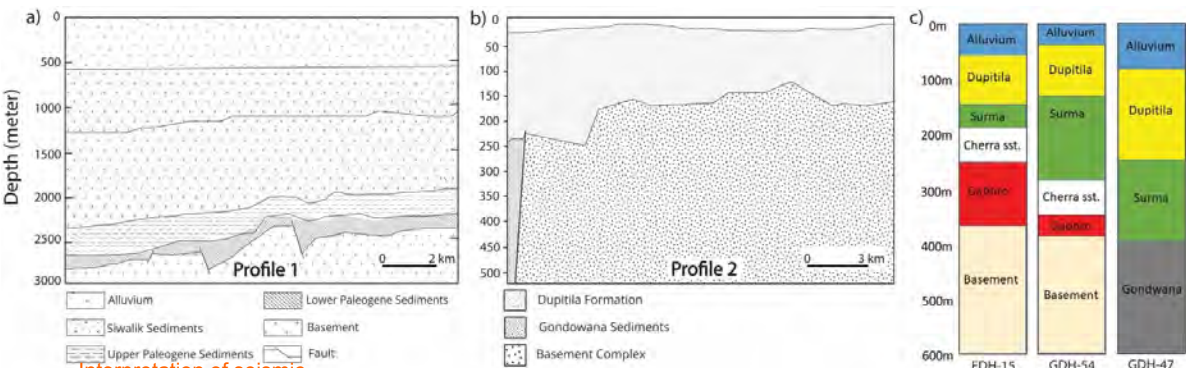
this is not seismic data but its interpretation

Interpretation of seismic

178
179 Figure 2: ~~Seismic~~ and drilling data used for integrated geophysical analysis in this study. (a) and (b) present
180 interpretations of the two seismic profiles analyzed. (c) shows the drilling log data, which correlates with the 2D
181 subsurface models and assists in spatial analysis. Refer to Figure 1b for their locations. Seismic profile 1 is from
182 Himalayan Foredeep region while profile 2 represents Rangpur Saddle. All the drilling logs are situated near the
183 highest observed magnetic anomaly in Pirganj, located in Northwestern Bangladesh.

Show drillhole locations on profiles and tell us which log corresponds to exactly which part of profiles

184
185 **3. Data and Methodology**
186
187 In this study, we apply an integrative analytical approach utilizing multiple geophysical datasets
188 for spatial analysis and 2-D subsurface modeling. Our primary datasets are potential field data,
189 specifically gravity and magnetic data, provided by the Geological Survey of Bangladesh (GSB).
190 We use Bouguer gravity data and total magnetic intensity data for our analysis. Topography data
191 used in our geophysical modeling are obtained from the online repository of the Scripps Institution
192 of Oceanography, which are derived from satellite altimetry (Smith and Sandwell, 1997).
193 Additionally, we incorporate interpretations of seismic images obtained from GSB to correlate our
194 findings from gravity and magnetic data. However, raw seismic images are unavailable, as private
195 entities originally collected them. To further refine our 2-D integrated modeling, we use drilling
196 data from three boreholes near our study area, also provided by GSB (see **Figure 1b** for the
197 locations).
198
199 For geophysical spatial analysis, we use gravity and magnetic anomaly maps. The Bouguer gravity
200 data from GSB are corrected for elevation. For the total magnetic intensity map, we apply a
201 differential reduction to the pole (RTP) to adjust the magnetic grid (Arkani-Hamed, 2007). This
202 correction involves computing magnetic inclination, declination, and total magnetic field values
203 based on the International Geomagnetic Reference Field (Alken et al., 2021) with a magnetic epoch
204 of 1980.
205

206 The next step in our spatial analysis methodology involves removing the regional trend from both
207 the gravity and magnetic data. This process, known as regional-residual separation, is essential for
208 isolating local anomalies by filtering out the broader, long-wavelength trends associated with
209 large-scale geological structures (Ashraf and Filina, 2023b; Kheyrollahi et al., 2021; Núñez-
210 Demarco et al., 2023). By removing these regional trends, we enhance the visibility of smaller-
211 scale or high-frequency anomalies, allowing subtle features and variations in the subsurface to be
212 highlighted more effectively. To remove regional anomalies, we apply an upward continuation of
213 1000 m to the Bouguer gravity data (**Figure 3a**). This approach simulates measuring the gravity
214 field at a higher elevation—1000 m in our case—effectively smoothing out high-frequency
215 anomalies associated with shallow or near-surface geological features (Balogun et al., 2023). For
216 RTP magnetic anomaly, we use a Gaussian filter to calculate the regional trend (**Figure 3b**). This
217 Gaussian filter acts as a low-pass filter, smoothing out high-frequency components in the dataset.
218 After extracting the regional anomaly from the potential field, we subtract it from the unfiltered
219 total anomaly, yielding the residual anomaly (**Figure 3**).
220
221 We apply several filters to the residual potential field data to enhance specific features and improve
222 interpretability (**Figure 3**). These filters involve various forms of derivative operations, which help
223 to highlight changes in the data that correspond to geological boundaries, faults, or other structural
224 details (Ibraheem et al., 2023; Ma et al., 2016; Nasuti et al., 2019; Núñez-Demarco et al., 2023).
225 For the residual RTP magnetic data, we apply and show two filters: the horizontal derivative and
226 the tilt derivative. The horizontal derivative filter, applied in x-direction (i.e., across the longitudes)
227 and y-direction (i.e., across the latitudes), accentuates lateral changes in the magnetic field, helping
228 to reveal abrupt variations. The tilt derivative filter, however, is especially effective as an edge
229 detector. It operates by combining both vertical and horizontal gradients, effectively highlighting
230 the edges of anomalous bodies. The tilt derivative produces values that tend toward zero over flat magnetically falt
231 regions, positive over rising areas, and negative over falling areas, creating a clear demarcation of
232 the edges of magnetic sources. As a result, this filter enhances the boundaries of anomalies and
233 helps pinpoint the locations and shapes of features with minimal distortion across varying depths
234 (Ashraf and Filina, 2023b; Pham and Oliveira, 2023). We apply the lineament mapping techniques
235 to map major structural boundaries from the filtered magnetic data (Ashraf & Filina, 2023a, 2023b;
236 Ogah & Abubakar, 2024; Zhang et al., 2024). Our approach focused on identifying gaps between
237 magnetic stripes, changes in the stripe orientation, and a significant reduction in stripe width. We
238 also calculate the analytical signals of the magnetic anomalies to highlight the areas with high
239 magnetizing amplitude (Nabighian, 1972; Roest and Pilkington, 1993) that may illuminate
240 magnetic mineral deposits (Mohamed et al., 2022). To calculate the analytical signal of the residual
241 magnetic data, we first compute the horizontal and vertical derivatives of the magnetic field in the
242 x, y, and z directions. The analytical signal was then derived by taking the square root of the sum
243 of the squares of these derivatives, yielding a map that represents the amplitude of the magnetic
244 field independent of direction and highlights the edges of magnetic sources. To validate our
245 interpretations, we cross-reference the magnetic lineaments with gravity data. Before validating
246 with gravity data, we filter the residual gravity data by applying the first vertical derivative and tilt
247 derivative to map major tectonic structures and delineate their boundaries.

248 The reason for using 1st vertical derivative in gravity to compare with reduced to pole magnetics is based in Poisson's theorem and also potential field theory. Look up Blakely's book and refer to original references.

249 We also develop 2-D integrated models of the subsurface to examine the variations in the physical
250 properties of the rocks (density and magnetic susceptibility). We build our models using the GM-
251 SYS module within the Geosoft software suite, employing a 2-D approximation (Geosoft, 2021).

252   The GM-SYS model is extended to +/- 30000 km (i.e., infinity) along the X-axis and 90 km along
253   the Z-axis to eliminate edge effects. By integrating gravity and magnetic data within this 2D
254   context, we can delineate major geological boundaries and assess regional structural trends with
255   sufficient accuracy for our research objectives. Our goal is to develop a simple subsurface structure
256   that satisfactorily aligns with gravity, magnetic, and logging data without introducing excessive
257   complexity that might overfit the potential field anomaly. Instead, we aim to replicate the general
258   pattern of the observed anomaly in our 2D modeling, seeking to generate computed anomalies
259   with comparable amplitude, wavelength, and phase to those observed in the potential fields.
260
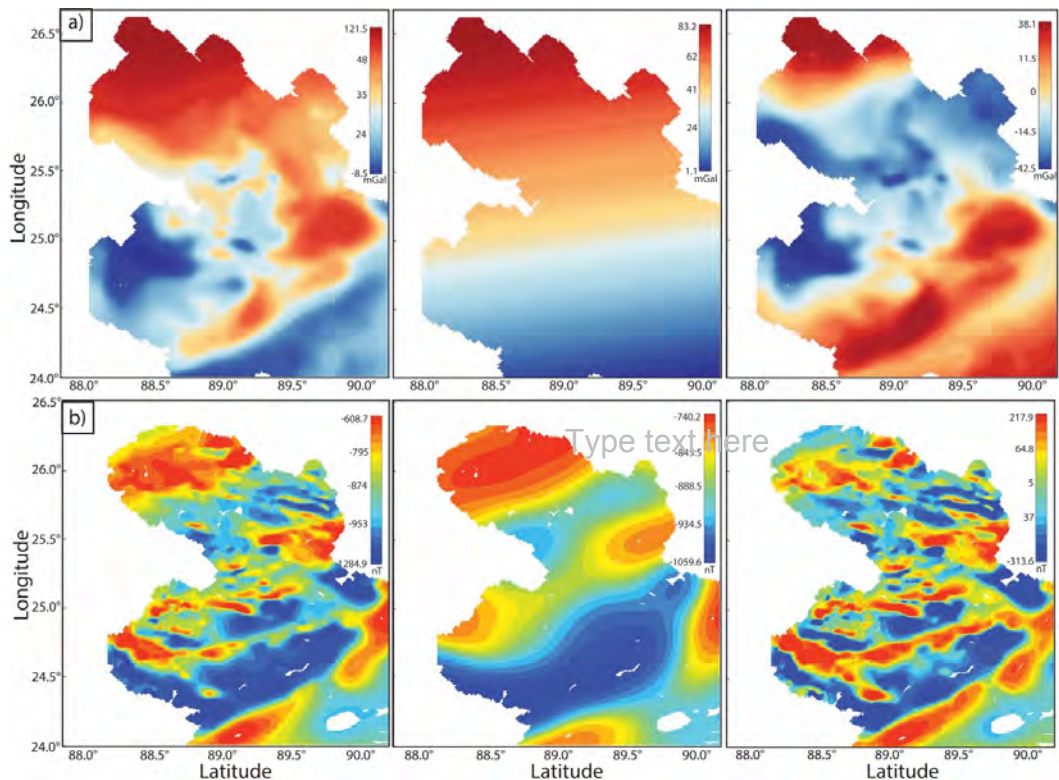
261
262
263   Figure 3: Potential field data maps of northwestern Bangladesh used in this study to analyze geological and tectonic
264   features. (a) Gravity anomaly maps: from left to right, the Bouguer gravity anomaly, regional Bouguer gravity anomaly
265   with 1000 m upward continuation, and residual Bouguer gravity anomaly. (b) Magnetic anomaly maps: from left to
266   right, the RTP total magnetic anomaly, regional magnetic anomaly after Gaussian filtering, and residual magnetic
267   anomaly. Important to show Rangpur Saddle boundaries on all these maps.

268
269   **4. Result** It is important to show the total field map and compare it with the RTP map to show that the regional anomalies are properly RTPed. It is important to specify inducing magnetic field inclination and declination used in the RTP. Also important to show that localized reverse remanently magnetized features exist on the map here and on Figure 4a (top)
270

271   **4.1 Integrated spatial analysis**

272

273   In this study, we first establish the regional tectonic structures of northwestern Bangladesh through
274   spatial analysis of multiple geophysical datasets. We utilize gravity, magnetic, seismic image

275 interpretations, and drilling log data to characterize the tectonic setup of this region. Our analysis
276 of residual magnetic and gravity anomalies reveals that the Rangpur Saddle exhibits distinct
277 geophysical characteristics compared to its northern counterpart, the Himalayan Foredeep region.
278 These differences are discernible in the long-wavelength or broad-scale geophysical signatures
279 across the two regions.

281 In the Himalayan Foredeep, north of 26°N latitude, we observe a high residual Bouguer gravity
282 anomaly, ranging from approximately 5 to 30 mGal. In contrast, the Rangpur Saddle, located south
283 of this latitude, is marked by a low residual Bouguer gravity anomaly, typically between -22 and
284 0 mGal. Similarly, the Rangpur Saddle shows lower residual RTP total magnetic anomalies,
285 ranging from 0 to 260 nT compared to mostly high magnetic anomalies in north (~ 0 to 215 nT).
286 The spatial patterns of these anomalies also differ across the regions. South of 26°N latitude, in
287 the Rangpur Saddle, the horizontal and tilt derivative magnetic anomalies show a predominance
288 of NW-SE trending magnetic lineaments. North of this latitude, in the Himalayan Foredeep, the
289 magnetic anomaly trend shifts predominantly to a SW-NE orientation. Additionally, In the vertical
290 and tilt derivatives of the gravity data, we observe the most pronounced high-gravity linear
291 anomaly patch trends NW-SE south of 26°N latitude, consistent with the magnetic anomaly trend
292 in this area. South of 26°30'N latitude, we see another linear high-gravity patch in the filtered
293 Bouguer gravity data trending NW-SE, indicating a different orientation than the other high-
294 gravity patch of the Rangpur Saddle region. These two high-gravity patches are also traceable in
295 the filtered magnetic anomalies, following the magnetic lineament mapping procedure.

297 Within the Rangpur Saddle region, we observe multiple semi-circular patterns characterized by
298 alternating magnetic highs and lows. From the RTP residual magnetic anomaly data, we identify
299 seven distinct patterns. The identification of these patterns follows several consistent criteria. First,
300 the alternating high and low anomalies are generally oriented in a north-south direction. Second,
301 each pattern features a magnetic high in the northern section and a corresponding low to the south.
302 Third, within each pattern, the size, area, and amplitude of the magnetic high and low anomalies
303 are comparable, contributing to a symmetrical structure. Mapping these magnetic patterns of
304 alternating highs and lows onto the filtered gravity maps reveals that they consistently lie near the
305 boundary between high and low gravity anomalies. While most of these magnetic patterns
306 (patterns 1, 4, 5, 6, and 7) intersect only one boundary, a few patterns (specifically patterns 2 and
307 3) touch boundaries on both sides.

309
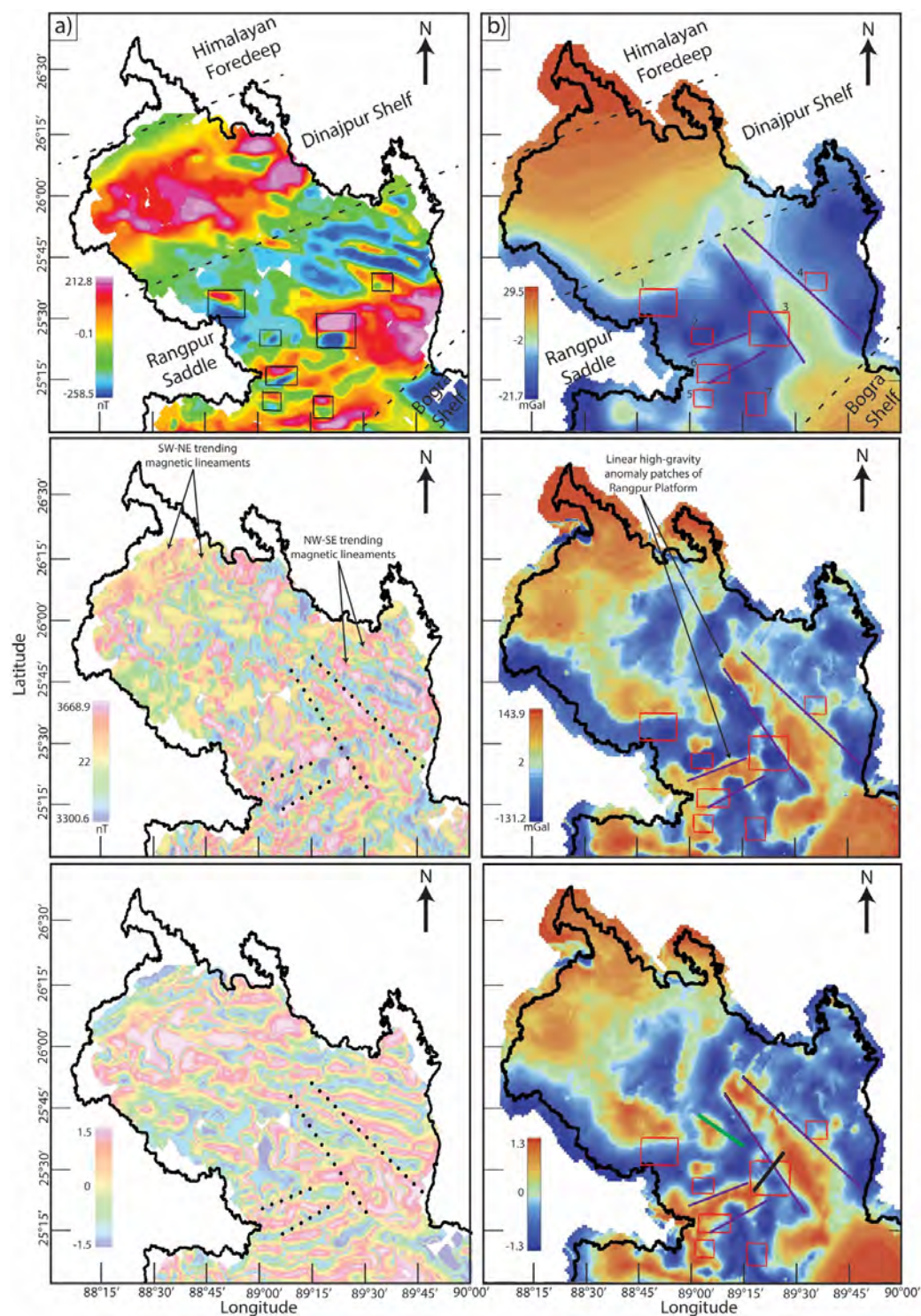
Once again: It is important to show the total field map and compare it with the RTP map to show that the regional anomalies are properly RTPed. It is important to specify inducding magnetic field inclination and declination used in the RTP. Also important to show that localized reverse remanently magnetized features exist on the map here and on Figure 4a (top)

Put numbers next to all boxes in the sub-figures.

Figure 4: a) Magnetic anomaly maps of northwestern Bangladesh. The top panel displays the residual RTP total magnetic anomaly, the middle panel shows the first horizontal derivative in the x-direction (across longitudes), and the bottom panel illustrates the tilt derivative. Black boxes highlight areas where semi-circular magnetic patterns of alternating highs and lows are observed. Dotted black lines in the middle and bottom panels indicate boundaries of high gravity regions. b) Bouguer gravity anomaly maps of northwestern Bangladesh. The top panel presents the residual Bouguer gravity anomaly, the middle panel shows the first vertical derivative, and the bottom panel displays *bipolar* the tilt derivative. High gravity regions are outlined by purple solid lines, and red boxes indicate areas with magnetic patterns of alternating highs and lows. The solid green line in the bottom panel represents seismic profile 2 from Figure 2. The thick solid black line shows the 2-D integrated modelling profile of Figure 5.

4.2 Integrated subsurface modeling

** The shortwavelength as well as long wavelendth misfit is too large, No matter what the regional may be the short wavelength modeled anomalies are much sharper suggesting their sources are too near-surface for the nature of the observed anomalies.

We develop a 2-D subsurface model utilizing gravity, magnetic, and drilling log data (**Figure 5**). *One would have to "add" a number of contrived sources to match the* The goal of this model is to approximate the observed anomalies on a local scale while aligning with the available drilling log information (**Figure 2c**). Importantly, we do not aim to achieve a *observed anomalies* precise fit between the observed data and calculated anomalies. This decision is driven by the fact that the observed potential field data are influenced by regional structures, and without sufficient seismic information, constructing a reliable regional model is not feasible. Instead, we focus on developing a simplified version of the subsurface model that reasonably fits the observed anomalies and drilling data.

To ground the 2-D model in reality, we incorporated available drilling log information (**Figure 2**). Based on these logs, the model includes five sedimentary layers above a crystalline basement. The shallowest layer is assigned as alluvium, extending to a depth of 50 meters or less. Beneath the alluvium, we sequentially include the Dupitila, Surma, and Cherra sandstone layers. The variable thickness of these sedimentary layers comes from the drilling log information, except for the Gondwana layer. The thickness of Gondwana is approximated based on the gravity fit. Below these layers, we model a mafic intrusion of gabbro, which occurs within fault structures that have developed within the underlying felsic basement.

Because of the large short wavelength misfit, you need to discuss what sort of sources would be needed to make up the difference (mis-fit).

The resulting model indicates that a horst and graben structure is the most plausible configuration when considering the regional geological context. This structural interpretation also provides a reasonable match to the observed geophysical anomalies. Additionally, based on information from drilling log GDH 47, we assign a layer of Gondwana sediments within the graben basin which is contributing to the low observed gravity in this region.

Densities in the model are derived from drilling data, reflecting the unique lithological characteristics of each unit. The alluvium, Dupitila, Surma, and Cherra Sandstone layers are modeled with densities of 2000, 2200, 2500, and 2670 g/cm³, capturing their progressive compaction and mineral composition. The Gondwana unit, enriched with coal deposits, exhibits a notably lower density of 2200 g/cm³, consistent with its organic-rich composition. Beneath these layers, the felsic basement and gabbroic intrusion stand out with densities of 2800 and 3000 g/cm³, highlighting their denser crystalline structure and mafic origins.

Between 400 and 800 meters depth, the gabbroic intrusion begins to follow the fault plane. The thickness of both the Gondwana layer and the underlying felsic basement is determined from the amplitude of the calculated gravity and magnetic anomalies. The thickness of the Gondwana layer influences the minimum value of the calculated gravity anomaly, while the amplitude of the

It is not just about the regional, but based on the magnetic gradient that source is deeper and gravity models need flanking low density bodies

358 magnetic anomaly helps determine the depth of the gabbroic intrusion. Notably, our calculated
359 anomalies are of high frequency. This occurs because our modeling does not incorporate all
360 regional structures; instead, it focuses only on local structures. As a result, the calculated anomalies
361 reflect primarily local or high-frequency potential field anomalies.

362

363 Our 2D subsurface model reveals two horst structures with a graben basin in the middle. We refer
364 to these as the eastern and western horsts based on their geographic locations. In the model, the
365 western horst structure is depicted as deeper, consistent with the observed gravity anomaly, which
366 shows lower gravity in the western horst compared to the eastern horst. Our model does not include
367 the *broader?* larger horst structure on the eastern side, which likely explains the discrepancy between the
368 calculated and observed anomalies over the eastern horst.

369

Is this the RTP magnetic field or total field intensity?

370

371
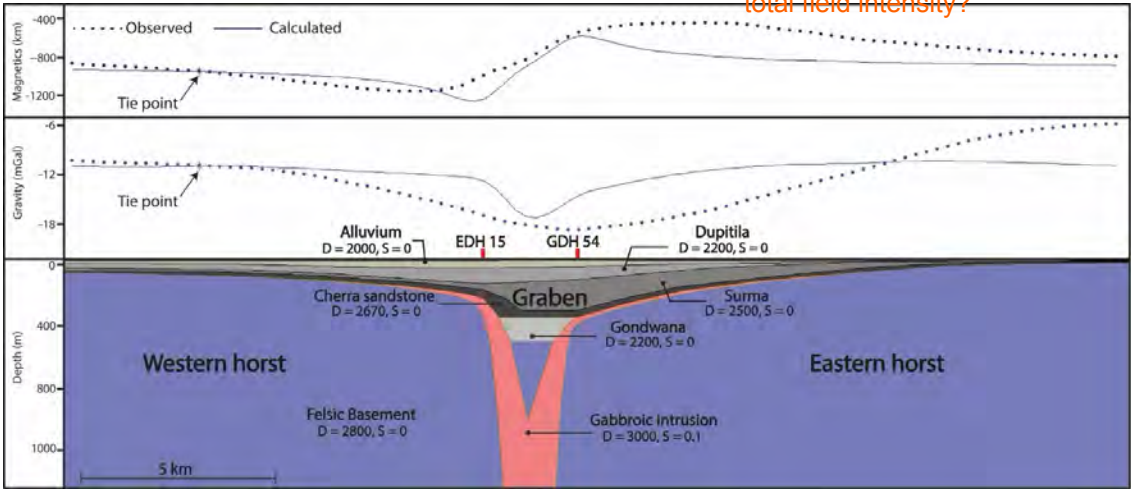
372 Figure 5: Integrated 2D geophysical model over the highest magnetic anomaly in northwestern Bangladesh. See Figure
373 1b and 4c for the location of the model profile. The top panel presents the magnetic anomaly, and the middle panel
374 shows the gravity anomaly, with observed (dotted) and calculated (solid) data. Tie points, marked by red stars, indicate
375 where the calculated anomalies are vertically shifted to align with the observed data. The bottom panel illustrates the
376 subsurface model, with geological units represented by distinct colors. 'D' denotes density (g/cm³), and 'S' denotes
377 magnetic susceptibility (SI units). The red vertical dashes show the location of the drilling logs used to constrain the
378 subsurface units.

379

380 ## 5. Discussion

381

382 ### 5.1 Basement structure

383

384 One of the primary goals of this paper is to understand the basement structure and tectonic setup
385 of the Rangpur Saddle. Our findings reveal significant differences in the basement structures of
386 the Rangpur Saddle compared to its northern counterparts, evident in both gravity and magnetic
387 data. A key distinction is the depth to basement between these regions (**Figure 1b**). Previous
388 studies consistently suggest that the basement depth in the Rangpur Saddle is shallower than in the
389 Dinajpur Shelf. However, those studies were based on limited seismic and drilling data. Our
390 results, however, indicate a more complex basement geometry than previously understood.

391 Filtered gravity and seismic data presented here suggest that the Rangpur Saddle region contains
392 both shallow and deep basement features (**Figure 4b**). Considering regional tectonics, we propose
393 that high gravity values correspond to shallow horst structures, while low gravity values indicate
394 deeper graben structures. However, the frequency of horsts and grabens is significantly lower in
395 the Rangpur Saddle compared to the northern Himalayan Foredeep and the Dinajpur Shelf (**Figure
396 2a** & **2b**). In the Rangpur region, we identified only two horsts of notable width and length. The
397 boundaries of these horst structures also appear as lineaments in the filtered magnetic data (**Figure
398 4a**), suggesting the presence of major structural boundaries.

400 Furthermore, differences in the directions of magnetic lineaments between the Rangpur Saddle
401 region and its northern counterparts—the Dinajpur Shelf and the Himalayan Foredeep—suggest
402 variations in paleo-tectonic stress orientation (**Figure 4a**, **6a** & **6b**). Existing literature
403 characterizes northwestern Bangladesh predominantly with extensional tectonics (Royhan Gani
404 and Mustafa Alam, 2003). Near the Himalayan Foredeep boundary, SW-NE trending magnetic
405 lineaments indicate a paleo-principal stress direction oriented NW-SE. Moving southward into the
406 Dinajpur Shelf, NW-SE trending magnetic lineaments become more common (**Figure 6b**),
407 pointing to a shift in the principal stress direction associated with extensional tectonics. In the
408 Rangpur Saddle, these NW-SE trending lineaments are even more frequent, especially in the
409 eastern part, indicating a greater intensity of paleo-tectonic stress in this region compared to the
410 Dinajpur Shelf. Based on traced magnetic and gravity lineaments, the stable platform can be
411 divided into four distinct zones (**Figure 6d**). In Zone 1, located in the northern part, lineaments
412 predominantly trend SW-NE, with only a few exceptions. Moving southward into Zone 2, there is
413 a mixture of two differently trending lineaments: SW-NE and NW-SE. In Zone 3, in the
414 easternmost section of the stable platform, lineaments primarily trend NW-SE, aligning with the
415 eastern horst. Finally, in Zone 4, the southernmost region, lineaments generally follow an SW-NE
416 trend, corresponding with the western horst. This subdivision highlights the complex nature of past
417 tectonic processes in this region.

419 We also identify seven semi-circular patterns of alternating magnetic highs and lows. When
420 mapped onto gravity data, these patterns consistently align with the boundaries between high and
421 low gravity patches, indicating the boundaries between horsts and grabens. Drilling log data near
422 the most prominent magnetic anomaly reveals the presence of gabbro, which may explain these
423 alternating magnetic highs and lows. Furthermore, these regions of alternating magnetic patterns
424 also spatially correlate with overall high magnetization (**Figure 6a**). We propose that these gabbro
425 formations resulted from intrusions along normal faults, formed by extensional tectonics, which
426 define the boundaries between horsts and grabens.
427

Remove any lineaments in part (d) taken from gravity gradient map in part (c).
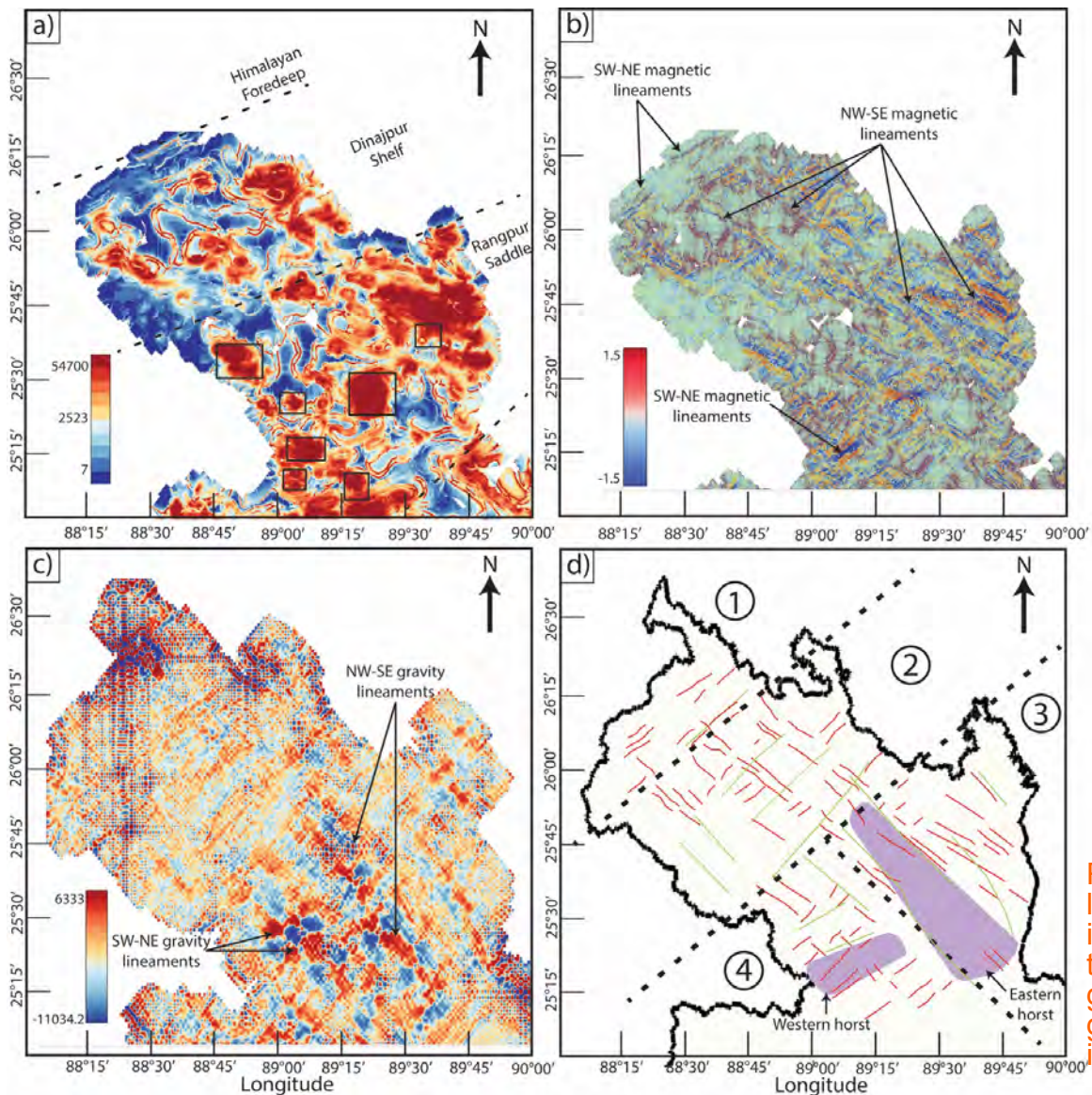
428
429 Figure 6: Filtered potential field maps of the northwestern stable platform region of Bangladesh, highlighting major
430 tectonic structures and boundaries. (a) Analytical signal map derived from the magnetic anomaly (methodology
431 detailed in Sect. 3), showing magnetization amplitudes across the region. Black boxes indicate areas of semi-circular
432 magnetic patterns with alternating highs and lows, as shown in Figure 4a. Dashed lines represent boundaries between
433 established tectonic subdivisions. (b) Total horizontal gradient map of the magnetic anomaly, calculated by applying
434 a first horizontal derivative filter in the X-direction, followed by a first horizontal derivative filter in the Y-direction.
435 (c) Total horizontal derivative of the residual gravity anomaly. (d) Map displaying traced magnetic lineaments (in red)
436 from 'b' and gravity lineaments (in green) from 'c'. Black dashed lines indicate regional subdivisions based on mapped
437 tectonic lineaments. Purple polygons mark horst structures in the Rangpur Saddle, interpreted from filtered gravity
438 data (refer to Figure 4b).
439

These speckled banded gravity features are caused by inadequate spacing gravity data. The residual map needs to be upward continued to a level where the derivative does not show these features.

5.2 Economic mineral potential

Our integrated spatial analysis and 2-D modeling indicate that the Rangpur Saddle hosts at least two significant horst and graben structures. The 2-D modeling results, corroborated by drilling log data, confirm the presence of gabbroic bodies along the normal faults within these structures (**Figure 7**). We propose that these gabbroic intrusions result from magmatic emplacement along extensional faults, consistent with processes typically observed during the early stages of continental breakup. The breakup process involved rifting events that progressively separated the Indian subcontinent from the other Gondwanaland constituents (Veevers, 2004). Key rifting episodes and magmatic activities, such as the formation of the Central Atlantic Magmatic Province and related tectonic movements, facilitated this separation (Thompson et al., 2019; Veevers, 2004). In such tectonic settings, normal faulting and rift-related subsidence create pathways for mafic magmas to ascend (Brune et al., 2023; Pirajno and Santosh, 2014; Ruppel, 1995), leading to the emplacement of gabbroic and other mafic intrusions within the crust (Magee et al., 2019).

Mafic magma intrusions are commonly observed along extensional fault planes in tectonically active regions worldwide. Troll et al. (2021) shows that in NW Scotland, Long Loch Fault acted as dynamic magma conduit with its movements facilitating the ascent of ultrabasic magmas. These magmas intruded along faults and fractures, leading to the destabilization and collapse of existing cumulate layers, forming extensive breccias. A study on Mesozoic gabbroic intrusions in the High Atlas Mountains highlights their emplacement along extensional faults during the rifting associated with the Central Atlantic Magmatic Province, where more than 50% of gabbro samples exhibit stable magnetization from magnetite which is identified as the primary component (Calvín et al., 2017). Fuller & Waters (1929) have extensively studied horsts and graben structures in southern Oregon where they found emplacement of volcanic and intrusive rocks are closely associated with extensional faulting. These normal faults and the resulting grabens provide pathways for magma to ascend and intrude, which is evident from the prevalence of rhyolitic, dacitic, and andesitic vents as well as basaltic dikes aligned with the faults.

Mafic intrusions along fault zones are often associated with magnetic mineral deposits, which can be economically significant as ore bodies (Zhou et al., 2005). For instance, magnetite deposits are found within mafic intrusions along the fault planes in Egypt, which exhibit high magnetic anomalies, facilitating their detection and delineation (Kharbish et al., 2022; Mousa et al., 2020). Also, in Central Iran, iron-bearing magnetic mineral deposits are observed to exhibit high magnetic and gravity anomalies (Kheyrollahi et al., 2021).

Based on current geochemistry data, the Rangpur Saddle holds significant potential for magnetic mineral ore deposits, driven by its mafic-ultramafic sequences and iron-rich dykes (Ameen et al., 2021). High Fe_2O_3 content in hornblendites and associated minerals like magnetite and ilmenite indicate strong magnetization. The tectonic setting, with extensive magmatic intrusions, provides ideal conditions for mineralization. These findings highlight the region as a promising target for future geophysical exploration of magnetic ore bodies.
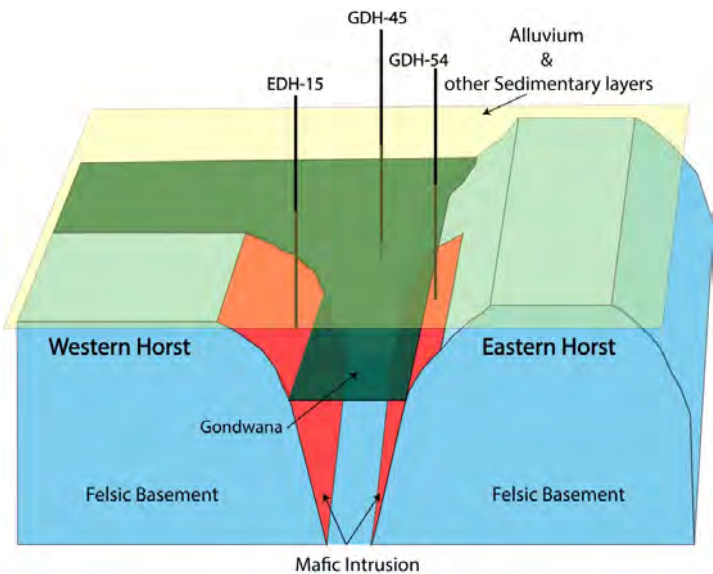
What is the age of the Gondawana sedimentary rocks? Needed for international audience.

Figure 7: 3D schematic diagram illustrating the tectonic structures in Pirganj, where the highest magnetic anomaly is observed in Bangladesh. The felsic basement, depicted in blue blocks, includes two horsts, as shown in Figure 5d. Possible mafic intrusions along the faults are indicated in red. Sedimentary layers are represented by a single horizontal layer in specific colors, with the graben basin likely filled with Gondwana sediments shown in green, and other sedimentary layers, including alluvium, shown in yellow. The approximate locations of the three drilling logs used in this study (refer to Figure 1b for their locations) are also indicated.

5.3 Limitations and Future Research

Compared to other regions globally, limited published research exists for our study area, restricting our ability to draw on established models and findings. Situated at the eastern edge of the Indian Shield, this area transitions into a different tectonic subdivision, creating a tectonic complexity that cannot be fully resolved with the available low-resolution data. The scarcity of high-resolution datasets, such as regional-scale seismic surveys, further limits our capacity to delineate regional structures accurately. Additionally, the available well log data are predominantly shallow, reaching depths of approximately 500 meters, which limits insights into deeper geological and tectonic features beyond 2 kilometers. Petrographic descriptions of the basement rocks are also rudimentary, as they are primarily based on a limited number of well logs, most of which were drilled before the 1990s, leaving significant gaps in our understanding of the area's deeper subsurface geology.

Future research in this region will focus on developing 3D models of the subsurface, providing a more detailed understanding of its geological structure. This effort will include creating a comprehensive dataset repository that incorporates historical seismic reflection data from private entities. Given the shallow depth of the region, high-resolution gravity and magnetic data will also be essential for a thorough analysis. This may require precision measurements through ground surveys to accurately collect gravity and magnetic data. The study area is characterized by complex tectonic structures shaped by a diverse tectonic history. While the current study has focused on the Rangpur Saddle, future research will expand to cover the entire northwestern part of Bangladesh,

meaning?

Are their regional or localized high resolution datasets available to conduct this research?

513 including the Himalayan Foredeep and the Eocene Hinge region, which represents a
514 Paleocontinental shelf. Such expanded coverage will provide deeper insights into the tectonic
515 evolution and geological complexity of the area.

516

517 **Conclusion**

518

519 This study provides a ~~comprehensive~~ geophysical investigation of the northwestern region of
520 Bangladesh, revealing its significant potential for mineral resource exploration. The integration of
521 gravity, magnetic, seismic, and drilling data has allowed us to identify key tectonic features, such
522 as gabbroic intrusions along extensional faults, some which may host ~~which suggest the presence of~~ valuable magnetic
523 mineral deposits. Despite the limitations in data resolution and coverage, our findings offer
524 important insights into the region's geological evolution and resource potential. Future work
525 should prioritize acquiring more detailed geophysical data and expanding drilling campaigns to
526 refine the understanding of subsurface structures and evaluate the feasibility of mineral extraction.
527 The Rangpur Saddle, as the shallowest part of the stable platform, emerges as a promising target
528 for future mineral exploration endeavors.

529

530 **Data availability**

531

532 All raw data can be provided by the corresponding authors upon request.

533

534 **Author contribution**

535

536 Mohammad Tawhidur Rahman Tushar was involved in conceptualization, methodology, software,
537 validation, formal analysis, investigation, resources, data curation, writing – original draft, writing
538 – review and editing, visualization. Asif Ashraf contributed to conceptualization, methodology,
539 software, validation, formal analysis, investigation, resources, data curation, writing – original
540 draft, writing – review and editing, and visualization. Md. Mahfuz Alam worked on software
541 development, validation, and formal analysis. Md Nasif Jamil contributed to writing – review and
542 editing and visualization. Saba Karim was involved in writing – review and editing and
543 visualization. Md. Shahjahan contributed to conceptualization, investigation, resources, project
544 administration, and supervision. Md. Anwar Hossain Bhuiyan was involved in writing – review
545 and editing, project administration, supervision, and funding acquisition.

546

547 **Competing interests**

548

549 The authors declare that they have no conflict of interest.

550

551 **Acknowledgment**

552

553 The gravity, magnetic, and seismic data, along with drilling information used in this study, were
554 graciously provided by the Geological Survey of Bangladesh (GSB), and the authors deeply
555 appreciate their support and collaboration. The authors also thank Asef Jamil Ajwad for his
556 assistance with computational facilities during the research. Special acknowledgment is made for
557 the Oasis Montaj classroom subscription and for the use of Geosoft Oasis Montaj v8.4 for data

558 processing and modeling. Finally, gratitude is extended to the Department of Geology, University
559 of Dhaka, for providing access to essential infrastructure and resources.
560

Financial support
562

563 This work was funded by the National Science and Technology Fellowship, awarded by the
564 Ministry of Science and Technology, Bangladesh.

565

References
567

568 Adebiyi, L. S., Eluwole, A. B., Fajana, A. O., Salawu, N. B., and Saleh, A.: Contrasting structures
569 of the Southern Benue trough and the contiguous crystalline basement as observed from high-
570 resolution aeromagnetic data, Sci Rep, 13, 21516, https://doi.org/10.1038/s41598-023-48639-8,
571 2023.

572 Ahamed, S., Hossain, D., and Alam, J.: Exploring Basement Surface relationship of north-west
573 Bengal Basin using satellite images and tectonic modeling,
574 https://doi.org/10.48550/ARXIV.2004.02734, 2020.

575 Akhtar, A.: Mineral resources and their economic significance in national development:
576 Bangladesh perspective, SP, 250, 127–134, https://doi.org/10.1144/GSL.SP.2005.250.01.12,
577 2005.

578 Alam, M.: Geology and depositional history of Cenozoic sediments of the Bengal Basin of
579 Bangladesh, Palaeogeography, Palaeoclimatology, Palaeoecology, 69, 125–139,
580 https://doi.org/10.1016/0031-0182(89)90159-4, 1989.

581 Alam, M., Alam, M. M., Curray, J. R., Chowdhury, M. L. R., and Gani, M. R.: An overview of
582 the sedimentary geology of the Bengal Basin in relation to the regional tectonic framework and
583 basin-fill history, Sedimentary Geology, 155, 179–208, https://doi.org/10.1016/S0037-
584 0738(02)00180-X, 2003.

585 Alken, P., Thébault, E., Beggan, C. D., Amit, H., Aubert, J., Baerenzung, J., Bondar, T. N., Brown,
586 W. J., Califf, S., Chambodut, A., Chulliat, A., Cox, G. A., Finlay, C. C., Fournier, A., Gillet, N.,
587 Grayver, A., Hammer, M. D., Holschneider, M., Huder, L., Hulot, G., Jager, T., Kloss, C., Korte,
588 M., Kuang, W., Kuvshinov, A., Langlais, B., Léger, J.-M., Lesur, V., Livermore, P. W., Lowes, F.
589 J., Macmillan, S., Magnes, W., Mandea, M., Marsal, S., Matzka, J., Metman, M. C., Minami, T.,
590 Morschhauser, A., Mound, J. E., Nair, M., Nakano, S., Olsen, N., Pavón-Carrasco, F. J., Petrov,
591 V. G., Ropp, G., Rother, M., Sabaka, T. J., Sanchez, S., Saturnino, D., Schnepf, N. R., Shen, X.,
592 Stolle, C., Tangborn, A., Tøffner-Clausen, L., Toh, H., Torta, J. M., Varner, J., Vervelidou, F.,
593 Vigneron, P., Wardinski, I., Wicht, J., Woods, A., Yang, Y., Zeren, Z., and Zhou, B.: International
594 Geomagnetic Reference Field: the thirteenth generation, Earth Planets Space, 73, 49,
595 https://doi.org/10.1186/s40623-020-01288-x, 2021.

596 Ameen, S. M. M., Wilde, S. A., Kabir, Md. Z., Akon, E., Chowdhury, K. R., and Khan, Md. S. H.:
597 Paleoproterozoic granitoids in the basement of Bangladesh: A piece of the Indian shield or an

exotic fragment of the Gondwana jigsaw?, Gondwana Research, 12, 380–387, https://doi.org/10.1016/j.gr.2007.02.001, 2007.

Ameen, S. M. M., Tapu, A.-T., and Hossain, M. S.: Precambrian Basement Rock of Bangladesh and Its Metallic Minerals, in: Bangladesh geosciences and resources potential, CRC Press Books, 25–54, 2021.

Anon: Geosoft, 2021.

Arkani-Hamed, J.: Differential reduction to the pole: Revisited, GEOPHYSICS, 72, L13–L20, https://doi.org/10.1190/1.2399370, 2007.

Ashraf, A. and Filina, I.: New 2.75-D gravity modeling reveals the low-density nature of propagator wakes in the Juan de Fuca plate, Tectonophysics, 869, 230127, https://doi.org/10.1016/j.tecto.2023.230127, 2023a.

Ashraf, A. and Filina, I.: Zones of Weakness Within the Juan de Fuca Plate Mapped From the Integration of Multiple Geophysical Data and Their Relation to Observed Seismicity, Geochem Geophys Geosyst, 24, e2023GC010943, https://doi.org/10.1029/2023GC010943, 2023b.

Balogun, O. B., Akereke, O. F., and Nwobodo, A. D.: Understanding the Constraints to the Correct Application of the Upward Continuation Operation in Gravity Data Processing, Pure Appl. Geophys., 180, 3787–3811, https://doi.org/10.1007/s00024-023-03348-1, 2023.

Brune, S., Kolawole, F., Olive, J.-A., Stamps, D. S., Buck, W. R., Buiter, S. J. H., Furman, T., and Shillington, D. J.: Geodynamics of continental rift initiation and evolution, Nat Rev Earth Environ, 4, 235–253, https://doi.org/10.1038/s43017-023-00391-3, 2023.

Calvín, P., Ruiz-Martínez, V. C., Villalaín, J. J., Casas-Sainz, A. M., and Moussaid, B.: Emplacement and Deformation of Mesozoic Gabbros of the High Atlas (Morocco): Paleomagnetism and Magnetic Fabrics, Tectonics, 36, 3012–3037, https://doi.org/10.1002/2017TC004578, 2017.

Chowdhury, K. R., Hossain, M. S., and Khan, M. S. H. (Eds.): Bangladesh geosciences and resources potential, First edition., CRC Press, Boca Raton, 610 pp., 2022.

Curray, J. R.: Geological history of the Bengal geosyncline, Journal of Association of Exploration Geophysicists, 12, 209–219, 1991.

Curray, J. R. and Moore, D. G.: Sedimentary and Tectonic Processes in the Bengal Deep-Sea Fan and Geosyncline, in: The Geology of Continental Margins, edited by: Burk, C. A. and Drake, C. L., Springer Berlin Heidelberg, Berlin, Heidelberg, 617–627, https://doi.org/10.1007/978-3-662-01141-6_45, 1974.

DeCelles, P. G.: Foreland Basin Systems Revisited: Variations in Response to Tectonic Settings, in: Tectonics of Sedimentary Basins, edited by: Busby, C. and Azor, A., Wiley, 405–426, https://doi.org/10.1002/9781444347166.ch20, 2011.

Filina, I., Biegert, E. K., Sander, L., Tschirhart, V., Bundalo, N., and Schiek-Stewart, C.: Integrated imaging: A powerful but undervalued tool, The Leading Edge, 38, 720–724, https://doi.org/10.1190/tle38090720.1, 2019.

Fuller, R. E. and Waters, A. C.: The Nature and Origin of the Horst and Graben Structure of Southern Oregon, The Journal of Geology, 37, 204–238, 1929.

Hasan, M. M., Monir, A., and Hassan, M.: Evaluating the Energy and Mineral Resources Prospect and Future Development in Bangladesh: A Review, https://doi.org/10.2139/ssrn.4484598, 2023.

Hendrickson, M. D.: Geologic interpretation of aeromagnetic and chemical data from the Oaks Belt, Wabigoon subprovince, Minnesota: implications for Au-rich VMS deposit exploration, Can. J. Earth Sci., 53, 176–188, https://doi.org/10.1139/cjes-2015-0141, 2016.

Hildenbrand, T. G.: Regional Crustal Structures and Their Relationship to the Distribution of Ore Deposits in the Western United States, Based on Magnetic and Gravity Data, Economic Geology, 95, 1583–1603, https://doi.org/10.2113/95.8.1583, 2000.

Hossain, I., Tsunogae, T., Rajesh, H. M., Chen, B., and Arakawa, Y.: Palaeoproterozoic U–Pb SHRIMP zircon age from basement rocks in Bangladesh: A possible remnant of the Columbia supercontinent, Comptes Rendus Geoscience, 339, 979–986, https://doi.org/10.1016/j.crte.2007.09.014, 2007.

Hossain, Md. S., Khan, Md. S. H., Chowdhury, K. R., and Abdullah, R.: Synthesis of the Tectonic and Structural Elements of the Bengal Basin and Its Surroundings, in: Tectonics and Structural Geology: Indian Context, edited by: Mukherjee, S., Springer International Publishing, Cham, 135–218, https://doi.org/10.1007/978-3-319-99341-6_6, 2019.

Ibraheem, I. M., Tezkan, B., Ghazala, H., and Othman, A. A.: A New Edge Enhancement Filter for the Interpretation of Magnetic Field Data, Pure Appl. Geophys., 180, 2223–2240, https://doi.org/10.1007/s00024-023-03249-3, 2023.

Jaffal, M., Goumi, N. E., Kchikach, A., Aïfa, T., Khattach, D., and Manar, A.: Gravity and magnetic investigations in the Haouz basin, Morocco. Interpretation and mining implications, Journal of African Earth Sciences, 58, 331–340, https://doi.org/10.1016/j.jafrearsci.2010.03.012, 2010.

Jain, A. K., Banerjee, D. M., and Kale, V. S.: Tectonics of the Indian Subcontinent, Springer International Publishing, Cham, https://doi.org/10.1007/978-3-030-42845-7, 2020.

Kabir, Z. M., Chowdhury, K. R., Akon, E., Kazi, A. I., and Ameen, S. M. M.: Petrogenetic Study of Precambrian Basement Rocks from Maddhapara, Dinajpur, Bangladesh, Bangladesh Geoscience Journal, 7, 1–18, 2001.

Khan, A. A. and Rahman, T.: An analysis of the gravity field and tectonic evaluation of the northwestern part of Bangladesh, Tectonophysics, 206, 351–364, https://doi.org/10.1016/0040-1951(92)90386-K, 1992.

Khan, F. H.: Geology of Bangladesh, 1991.

Kharbish, S., Eldosouky, A. M., and Amer, O.: Integrating mineralogy, geochemistry and aeromagnetic data for detecting Fe–Ti ore deposits bearing layered mafic intrusion, Akab El-Negum, Eastern Desert, Egypt, Sci Rep, 12, 15474, https://doi.org/10.1038/s41598-022-19760-x, 2022.

Kheyrollahi, H., Alinia, F., and Ghods, A.: Regional magnetic and gravity structures and distribution of mineral deposits in Central Iran: Implications for mineral exploration, Journal of Asian Earth Sciences, 217, 104828, https://doi.org/10.1016/j.jseaes.2021.104828, 2021.

Ma, G., Huang, D., and Liu, C.: Step-Edge Detection Filters for the Interpretation of Potential Field Data, Pure Appl. Geophys., 173, 795–803, https://doi.org/10.1007/s00024-015-1053-6, 2016.

Magee, C., Ernst, R. E., Muirhead, J., Phillips, T., and Jackson, C. A.: Magma transport pathways in large igneous provinces: lessons from combining field observations and seismic reflection data, in: Dyke Swarms of the World: A Modern Perspective, 45–85, 2019.

Masum, M., Hoque, M. N., Akbar, M. A., Mahmud, Z., Rana, M. S., Razzaque, M. A., and Amin, M. A.: Geology and Precambrian Banded Iron Formation formed at Rangpur Platform in Bangladesh, International Journal Of Engineering Research And Development, 17, 43–57, 2021.

McCafferty, A. E., Stoeser, D. B., and Van Gosen, B. S.: Geophysical interpretation of U, Th, and rare earth element mineralization of the Bokan Mountain peralkaline granite complex, Prince of Wales Island, southeast Alaska, Interpretation, 2, SJ47–SJ63, https://doi.org/10.1190/INT-2014-0010.1, 2014.

Mohamed, A., Abdelrady, M., Alshehri, F., Mohammed, M. A., and Abdelrady, A.: Detection of Mineralization Zones Using Aeromagnetic Data, Applied Sciences, 12, 9078, https://doi.org/10.3390/app12189078, 2022.

Moon, J. W.: The Mineral Industry of Bangladesh, U.S. Geological Survey, 2022.

Morgan, J. P. and McINTIRE, W. G.: QUATERNARY GEOLOGY OF THE BENGAL BASIN, EAST PAKISTAN AND INDIA, Geol Soc America Bull, 70, 319, https://doi.org/10.1130/0016-7606(1959)70[319:QGOTBB]2.0.CO;2, 1959.

Mousa, S. A. W., Abdel Nabi, S. H., Araffa, S. A. S., Mansour, S. A., and Al Deep, M. A. I.: Geophysical exploration of titanomagnetite ore deposits by geomagnetic and geoelectric methods, SN Appl. Sci., 2, 444, https://doi.org/10.1007/s42452-020-2206-5, 2020.

Nabighian, M. N.: THE ANALYTIC SIGNAL OF TWO-DIMENSIONAL MAGNETIC BODIES WITH POLYGONAL CROSS-SECTION: ITS PROPERTIES AND USE FOR AUTOMATED ANOMALY INTERPRETATION, GEOPHYSICS, 37, 507–517, https://doi.org/10.1190/1.1440276, 1972.

704 Nasuti, Y., Nasuti, A., and Moghadas, D.: STDR: A Novel Approach for Enhancing and Edge
705 Detection of Potential Field Data, Pure Appl. Geophys., 176, 827–841,
706 https://doi.org/10.1007/s00024-018-2016-5, 2019.

707 Núñez-Demarco, P., Bonilla, A., Sánchez-Bettucci, L., and Prezzi, C.: Potential-Field Filters for
708 Gravity and Magnetic Interpretation: A Review, Surv Geophys, 44, 603–664,
709 https://doi.org/10.1007/s10712-022-09752-x, 2023.

710 Ogah, A. J. and Abubakar, F.: Solid mineral potential evaluation using integrated aeromagnetic
711 and aeroradiometric datasets, Sci Rep, 14, 1637, https://doi.org/10.1038/s41598-024-52270-6,
712 2024.

713 Pham, L. T. and Oliveira, S. P.: Edge Enhancement of Magnetic Sources Using the Tilt Angle and
714 Derivatives of Directional Analytic Signals, Pure Appl. Geophys., 180, 4175–4189,
715 https://doi.org/10.1007/s00024-023-03375-y, 2023.

716 Pirajno, F. and Santosh, M.: Rifting, intraplate magmatism, mineral systems and mantle dynamics
717 in central-east Eurasia: An overview, Ore Geology Reviews, 63, 265–295,
718 https://doi.org/10.1016/j.oregeorev.2014.05.014, 2014.

719 Rahman, Md. M. and Ullah, S. E.: Inversion of Gravity Data for Imaging of a Sediment-basement
720 Interface: A Case Study in the Northwestern Part of Bangladesh, Pure Appl. Geophys., 166, 2007–
721 2019, https://doi.org/10.1007/s00024-009-0530-1, 2009.

722 Reimann, K. U. and Hiller, K.: Geology of Bangladesh, 1993.

723 Roest, W. R. and Pilkington, M.: Identifying remanent magnetization effects in magnetic data,
724 GEOPHYSICS, 58, 653–659, https://doi.org/10.1190/1.1443449, 1993.

725 Roy, A. B. and Chatterjee, A.: Tectonic framework and evolutionary history of the Bengal Basin
726 in the Indian subcontinent, Current Science, 109, 271–279, 2015.

727 Royhan Gani, M. and Mustafa Alam, M.: Sedimentation and basin-fill history of the Neogene
728 clastic succession exposed in the southeastern fold belt of the Bengal Basin, Bangladesh: a high-
729 resolution sequence stratigraphic approach, Sedimentary Geology, 155, 227–270,
730 https://doi.org/10.1016/S0037-0738(02)00182-3, 2003.

731 Ruppel, C.: Extensional processes in continental lithosphere, J. Geophys. Res., 100, 24187–24215,
732 https://doi.org/10.1029/95JB02955, 1995.

733 Smith, W. H. F. and Sandwell, D. T.: Global Sea Floor Topography from Satellite Altimetry and
734 Ship Depth Soundings, Science, 277, 1956–1962, https://doi.org/10.1126/science.277.5334.1956,
735 1997.

736 Sundararajan, N.: A General Perspective on Geophysical Methods in Mineral Exploration, in: On
737 a Sustainable Future of the Earth's Natural Resources, 53–83, 2012.

738   Thompson, J. O., Moulin, M., Aslanian, D., De Clarens, P., and Guillocheau, F.: New starting
739   point for the Indian Ocean: Second phase of breakup for Gondwana, Earth-Science Reviews, 191,
740   26–56, https://doi.org/10.1016/j.earscirev.2019.01.018, 2019.

741   Troll, V. R., Mattsson, T., Upton, B. G. J., Emeleus, C. H., Donaldson, C. H., Meyer, R., Weis, F.,
742   Dahrén, B., and Heimdal, T. H.: Fault-Controlled Magma Ascent Recorded in the Central Series
743   of the Rum Layered Intrusion, NW Scotland, Journal of Petrology, 61, egaa093,
744   https://doi.org/10.1093/petrology/egaa093, 2021.

745   Uddin, A. and Lundberg, N.: Unroofing history of the eastern Himalaya and the Indo-Burman
746   ranges; heavy-mineral study of Cenozoic sediments from the Bengal Basin, Bangladesh, Journal
747   of Sedimentary Research, 68, 465–472, https://doi.org/10.2110/jsr.68.465, 1998.

748   Valdiya, K. S.: The Making of India, Springer International Publishing, Cham,
749   https://doi.org/10.1007/978-3-319-25029-8, 2016.

750   Veevers, J. J.: Gondwanaland from 650–500 Ma assembly through 320 Ma merger in Pangea to
751   185–100 Ma breakup: supercontinental tectonics via stratigraphy and radiometric dating, Earth-
752   Science Reviews, 68, 1–132, https://doi.org/10.1016/j.earscirev.2004.05.002, 2004.

753   Zhang, H., Greco, F., Sacek, V., Geng, M., and Liu, P.: Editorial: Applications of gravity
754   anomalies in geophysics, Front. Earth Sci., 12, 1349161,
755   https://doi.org/10.3389/feart.2024.1349161, 2024.

756   Zhang, S., Li, Z.-X., Evans, D. A. D., Wu, H., Li, H., and Dong, J.: Pre-Rodinia supercontinent
757   Nuna shaping up: A global synthesis with new paleomagnetic results from North China, Earth and
758   Planetary Science Letters, 353–354, 145–155, https://doi.org/10.1016/j.epsl.2012.07.034, 2012.

759   Zhou, M.-F., Robinson, P. T., Lesher, C. M., Keays, R. R., Zhang, C.-J., and Malpas, J.:
760   Geochemistry, Petrogenesis and Metallogenesis of the Panzhihua Gabbroic Layered Intrusion and
761   Associated Fe–Ti–V Oxide Deposits, Sichuan Province, SW China, Journal of Petrology, 46,
762   2253–2280, https://doi.org/10.1093/petrology/egi054, 2005.

763